In situ extracting organic-bound calcium: a novel approach to mitigating organic fouling in forward osmosis treating wastewater via gradient diffusion thin-films

Ling Li[a], Xinhua Wang[a,*], Ming Xie[b], Zhiwei Wang[c], Xiufen Li [a,*], Yueping Ren[a]

[a] Jiangsu Key Laboratory of Anaerobic Biotechnology, School of Environmental and Civil Engineering, Jiangnan University, Wuxi, P.R. China

[b] Institute for Sustainability and Innovation, College of Engineering and Science, Victoria University, Melbourne, Australia

[c] State Key Laboratory of Pollution Control and Resource Reuse, School of Environmental Science and Engineering, Tongji University, Shanghai, P.R. China

[*] Corresponding author. E-mail: xhwang@jiangnan.edu.cn (X. Wang), xfli@jiangnan.edu.cn (X. Li); Tel: +86-510-85326516.

Abstract

Forward osmosis (FO) has gained increasing interests in wastewater treatment and reclamation. However, membrane fouling has become one major obstacle hindering FO application. A novel mitigation approach for FO membrane fouling via *in situ* extracting Ca^{2+} binding with the organic foulants using the gradient diffusion thin-films (DGT) was proposed in this study. The DGT could effectively adsorb the Ca^{2+} binding with the sodium alginate via the chelation of the Chelex functional groups, and its adsorption amount of Ca^{2+} correspondingly increased as a function of the Ca^{2+} concentration in the feed solution. Owing to the extraction of Ca^{2+} from the fouling layer by the DGT, the FO membrane fouling was effectively mitigated evident by significant enhancement of water flux, and at the same time, foulants became easily removed by physical cleaning. The alleviation of FO membrane fouling by the DGT could be attributed to the fact that the structure of the fouling layer became more porous and looser after *in situ* removing Ca^{2+} from the alginate-Ca^{2+} gel networks. The feasibility of fouling control strategy via *in situ* removing Ca^{2+} binding with the foulants in the fouling layer was demonstrated, which provides new insights into fouling control mechanisms during FO treating wastewater.

Keywords: forward osmosis, membrane fouling, organic foulants, calcium, gradient diffusion thin-films, wastewater treatment

1. Introduction

Forward osmosis (FO) process has raised increasing attentions as a promising technology for wastewater treatment and reclamation (Liu and Mi, 2012; Zhao et al., 2012; Lutchmiah et al., 2014). FO process utilizes osmotic pressure gradient as driving force to extract water molecule from the feed solution (FS) through the FO membrane to the draw solution (DS). Compared to the pressure-driven membrane processes including reverse osmosis (RO) and nanofiltration (NF), the osmotic pressure-driven FO process has several advantages such as lower energy consumption (if no need to regenerate the draw solution), higher water recovery, and superior water flux stability against fouling (McGinnis and Elimelech, 2007; Mi and Elimelech, 2010; Gu et al., 2013; McGovern and Lienhard, 2014; Shaffer et al., 2015; Tow and Lienhard, 2016; Siddiqui et al., 2018). Nevertheless, similar to other membrane processes, membrane fouling remains a major obstacle hindering a wider application of FO to complex waste streams, and its combined bioreactor (e.g., osmotic membrane bioreactor (OMBR) and anaerobic membrane bioreactor (AnOMBR)) in wastewater treatment and reclamation (Mi and Elimelech, 2010; She et al., 2016; Wang et al., 2016a, 2017, 2018a, 2019; Luo et al., 2017).

Fouling occurs when solutes or particles in the feed deposit onto surfaces or into pores of the FO membrane (Liu and Mi, 2012), which not only enhances the resistance of FO membrane but also increases the external concentration polarization (ECP) (Wang et al., 2014; Motsa et al., 2015). FO membrane fouling can be classified as organic, inorganic, microbial (biofouling) and colloidal fouling (Liu and Mi, 2012; Wang et al., 2014; Sun et al., 2016). Abundant and ubiquitous organic substances in the feed water such as, natural organic matters, alginates, and proteins, induce severe fouling on FO membrane surface (Mi and Elimelech, 2008, 2010; Xie et al., 2013). In addition,

inorganic species not only tend to directly precipitate onto the FO membrane surface but also interact with the organic foulants by bridging negatively charged functional groups (Sobeck and Higgins, 2002; Boo et al., 2012). Moreover, microorganisms especially bacteria can adhere to the FO membrane and subsequently form a biofilm (Yoon et al., 2013; Kwan et al., 2015), and colloidal fouling is owing to the deposition of colloidal particles (Liu and Mi, 2012). Correspondingly, FO membrane fouling has been extensively investigated using single model foulant such as alginate, bovine serum albumin (BSA), gypsum and *Pseudomonas* aeruginosa (Mi and Elimelech, 2008; Arkhangelsky et al., 2012; Kwan et al., 2015). Compared with other fouling types, organic fouling is more complicated, not only because specific interactions between chemical functional groups on the FO membrane surface and those of the organic foulants may occur, but it was also found to be affected by the ionic composition of the feed solution (Li and Elimelech, 2006). As a result, previous studies on FO membrane fouling are focused on organic fouling (Li and Elimelech, 2006; Mi and Elimelech, 2010; Liu and Mi, 2012; Motsa et al., 2015; Zheng et al., 2018). In these studies, it has been demonstrated that organic fouling of FO membrane is enhanced by divalent cations, i.e., forming a dense, cross-linked organic fouling layer, and consequently resulting in a rapid flux decline (Li and Elimelech, 2006). It is hypothesized that if the divalent cations can be extracted from the foulants on the FO membrane surface, the organic fouling layer might become loose and subsequently easily remove by a simply physical cleaning.

Diffusive gradients in thin-films (DGT) has become an attractive technology with a wide range of applications, including water quality monitoring, dynamic processes and bioavailability in waters and soils (Perez et al., 2009; Town et al., 2009; Schintu et al., 2010). The DGT technology can be used to adsorb most metals (e.g., Al, Zn, Cu) in water and soil based on Fick's first law of diffusion

(Zhang and Davison, 1995; Degryse et al., 2009; Guan et al., 2015). It consists of the innermost resin layer, a specific thickness of the diffusion gel, and a membrane filter (Zhang et al., 1998; Guan et al., 2015). The diffusive gel provides a controlled medium through which ions migrate before being adsorbed on the resin, and the resin layer is used to absorb the enriched target ions (Sherwood et al., 2009). The adsorbent material in the resin layer has a strong binding ability to metal (metalloid) ions, and its target in the solution is adsorbed immediately after passing through the diffusion gel to the resin layer (Davison and Zhang, 2012). The DGT technology has the advantages of simplicity, *in situ* and quantitative concentration of metals and non-metallic elements, as well as morphological analysis by simulating the absorption process of organisms (Zhang and Davison, 2015).

We are inspired by the successful extraction of metal ions from soils/sediments using DGT, where the metal ions in soils/sediments are effectively transferred to the DGT and subsequently to the liquid phase. In this study, applying the DGT technology for *in situ* adsorbing the divalent cations binding with the organic foulants from the FO membrane surface was attempted, thereby for mitigating membrane fouling and facilitating the subsequent membrane cleaning. Studies on applying the DGT technology for controlling organic fouling of FO membrane were rare in current literature. The objective of this study is to evaluate the feasibility of alleviating the FO membrane fouling through *in situ* removing the Ca^{2+} combined with the organic foulants by the DGT technology.

2. Materials and methods

2.1 Experimental set-up

Fouling profile of the FO membrane was evaluated in a bench-scale filtration system, as schematically shown in Fig. S1, Supporting Information. This test system included a cross-flow

membrane cell with two symmetric flow channels (each of 85 mm × 39 mm × 2 mm in dimension). Membrane coupons were placed in the membrane cell between the two channels for the DS and FS, respectively. Two peristaltic pumps (Longer Precision Pump, China) were used to pump the DS and FS into the separate closed loops. The cross-flow velocity in both channels of the membrane cell was constant at 1.3 mm/s. Both DS and FS were kept at room temperature (25 ± 2 °C). Change in the weight of FS was monitored by a digital balance (Mettler Toledo, China) and recorded in a computer by a data acquisition software (Mettler Toledo, China), which was converted into changes in water flux of FO membrane.

2.2 Operating conditions

Thin film composite (TFC) polyamide FO membrane (supplied by Hydration Technology Innovations) was used in this study. The TFC membrane has an asymmetric structure including a dense active layer (AL) and a porous support layer (SL) embedded with a polyester mesh. The water permeability coefficients (A) and salt permeability coefficients (B) of the TFC FO membrane were 4.9×10^{12} m/(s Pa) and 0.95×10^{-7} m/s, respectively. Membrane samples were stored in deionized (DI) water at 4 °C and soaked in DI water at room temperature for 24 h before each test.

A 4 M NaCl solution was used as the DS in both fouling and baseline experiments. Sodium alginate (75-100 kDa) was selected as the model organic foulant. The baseline experiment was conducted before the fouling experiment with the DI water as the FS and the 4 M NaCl as the DS. In order to evaluate the adsorption efficiency of DGT for Ca^{2+} binding with the sodium alginate, the FO membrane was fouled by the sodium alginate and $CaCl_2$ in sequence, which was different from the previous fouling protocol (Liu and Mi, 2012; Motsa et al., 2015). The procedure of the FO membrane fouling tests was conducted as follows (see for Fig. S2, Supporting Information). Firstly,

a new FO membrane coupon was sealed in the FO cell with active layer facing FS, and then a baseline experiment was performed for 4 h to obtain the initial flux of the FO membrane. After that, the fouling tests were started with 2 L of FS and DS. With regard to the single organic fouling, the fouling filtration was operated for 48 h; while the enhanced organic fouling filtration was conducted with a $CaCl_2$ solution for 24 h after the single organic fouling experiments operated for 24 h. As for the single organic fouling, the FS consisted of 200 mg/L sodium alginate, 20 mM NaCl, 20 mM Na_2SO_4 and 1 mM $NaHCO_3$, while the FS was changed into the $CaCl_2$ solution with three concentration levels of 1, 15 and 35 mM, respectively, for the tests of enhanced organic fouling by the Ca^{2+}. All the chemicals were obtained from Sigma-Aldrich (Shanghai, China).

2.3 DGT adsorption and evaluation

The DGT adsorption experiments were conducted after the fouling tests. As schematically shown in Fig. 1, the DGT device included the membrane filter, the diffusive gel strip and the resin layer (DGT Research Ltd., UK). During the adsorption experiments, the fouled FO membranes were attached to the membrane filter for 48 h. After that, the resin layer made of Chelex-100 strip (a commonly used chelating resin) was removed into the 1 M HNO_3 eluent for 24 h. Meanwhile, the remaining foulants were removed from the FO membrane surface by ultrasound (35 Hz，15 min) (Pendashteh et al., 2011). The extracted and ultrasound-extractable remaining Ca^{2+} concentrations were measured by an Atomic Absorption Spectrometer (Shimadzu Tokyo, Japan).

Fig. 1

In order to evaluate the adsorption efficiency of the DGT, the extracted Ca^{2+} concentration was converted into the adsorption amount on the Chelex gel strip according to the below equation.

$$M = C_e V_e / f_e \quad (1)$$

where M is the amount of Ca^{2+} absorbed on the Chelex gel strip, C_e is the concentration of Ca^{2+} in the eluent, V_e is the volume of the eluent (50 mL in this study), and f_e is the elution efficiency (0.8 for Ca^{2+}) (Zhang and Davison, 1995; Warnken et al., 2006; Montero et al., 2012).

The ultrasound-extractable remaining Ca^{2+} amount on the fouled FO membrane was correspondingly converted by the following equation.

$$M_R = C_R V_R \quad (2)$$

where M_R is the amount of Ca^{2+} remained on the fouled membrane surface, C_R is the concentration of the ultrasound-extractable remaining Ca^{2+}, and V_R is the volume of the dissolved residual foulants (100 mL in this study).

Based on the calculation of M and M_R, the adsorption efficiency (η) was obtained according to the below equation.

$$\eta\ (\%) = M/(M+M_R) \times 100\% \quad (3)$$

2.4 Analytical method

Water flux through the FO membrane was obtained based on the weight change of the FS. After the fouling tests and the DGT adsorption experiments, the water flux of the fouled and adsorbed FO membranes were determined by the FO cell for 4 h with the DI water as the FS and the 4 M NaCl as the DS. In order to eliminate the impacts of initial water flux (also measured by the FO cell) for different FO membranes, a normalized water flux was used for characterizing the fouled and adsorbed FO membranes. It was obtained through the determining flux dividing by the initial flux before fouling tests.

The conductivity of the FS was monitored and recorded by a conductivity meter (EC300A, YSI, USA). The FO membrane samples were obtained by randomly cutting from the fouled FO

177 membranes removed from the FO cell. An energy diffusive X-ray (EDX) analyzer (Su-8020, Hitachi,
178 Japan) and a field-emission scanning electron microscopy (FE-SEM) (Su-8020, Hitachi, Japan)
179 were applied for capturing the element compositions and surface images of the fouled and adsorbed
180 FO membrane samples, respectively. Prior to SEM and EDX observations, all FO membrane
181 samples were prepared by freezing the membrane at -80 °C in a chiller for 2 h followed by freeze
182 drying at -48 °C for 6 h using a freeze dryer (FreeZone 25, Labconco, Czech Republic). The
183 distributions of polysaccharides on the fouled and adsorbed FO membrane samples were analyzed
184 by the confocal laser scanning microscopy (CLSM) (LSM 710, ZEISS, Germany). The probe of
185 Calcofluor white (CW) (0.3 g/L) was used to stain the polysaccharides on the FO membrane samples.
186 After the labeling process, the samples were incubated for 30 min at room temperature in the dark,
187 and then were washed twice with phosphate buffered saline (PBS) solution to remove the extra
188 probes. The stained FO membrane samples were characterized by the CLSM at the
189 excitation/emission wavelengths of 405 nm/410-480 nm. Three-dimensional reconstructions were
190 obtained with ZEISS confocal software (ZEN 2012), and the images were analyzed by softwares of
191 PHLIP (Version 0.7) and Image J (NIH, Bethesda, MD, USA) to calculate the quantitative
192 parameters including average amount of polysaccharide, mean thickness and porosity (Mueller et
193 al., 2006; Yu et al., 2011; Yuan et al., 2015; Wang, et al., 2016b).

194 All experiments are repeated at least three times for statistics. The data shown in tables and
195 figures is expressed as means with standard deviations.

196 **3. Results and discussion**

197 *3.1 Water flux profile*

198 Water flux profiles of FO membranes at different fouling conditions are shown in Fig. 2. Water

199 flux of FO membrane decreased with the extension of the operating time regardless of the
200 composition of the FS. However, the profile for FO membrane water flux decline was highly
201 dependent on the foulants composition in the FS. Compared with the single organic fouling only
202 induced by the sodium alginate, the flux decline became severer when the Ca^{2+} was added into the
203 FS. In addition, the rate for water flux decline was accelerated with an increase of the Ca^{2+}
204 concentration. Moreover, the cleaning experiments on the fouled FO membranes at different fouling
205 conditions were conducted by the backwashing in the FO cell for 0.5 h with the 0.5 M NaCl as the
206 FS and the DI water as the DS according to previous literatures (Mi and Elimelech, 2010; Motsa et
207 al., 2017) . The results indicated that the alginate fouling became difficult to clean when Ca^{2+} was
208 present in the influent, e.g., the increasing rate of the normalized water flux was about 20% for the
209 single organic fouling only induced by the sodium alginate while it became less than 5% for the
210 organic fouling induced by the sodium alginate and 35 mM Ca^{2+}. These facts clearly showed that
211 Ca^{2+} aggravated the organic fouling of FO membrane, which was consistent with previous literature
212 (Liu and Mi, 2012; Motsa et al., 2015; Charfi, et al., 2017). This phenomenon could be attributed to
213 the fact that Ca^{2+} and alginate form complexes with unique structure, thereby leading to a high
214 density gel network (Van den Brink et al., 2009; Wang and Waite, 2009).

215 Fig. 2

216 *3.2 DGT approach effectively extracted calcium from fouling layer*

217 After the fouling tests of the FO membranes, Ca^{2+} was extracted from the fouled FO
218 membranes by the DGT technology. The normalized membrane flux of the fouled FO membranes
219 before and after DGT adsorptions are summarized in Fig. 3 (a). Specifically, there were no changes
220 in the normalized water flux of the fouled FO membrane with only alginate sodium before and after

221 the DGT adsorption, indicating that the DGT had no impacts on the single organic fouling of FO
222 membrane. By contrast, the normalized water flux had a significant increase after the DGT
223 adsorption for the organic fouling enhanced by Ca^{2+}, suggesting an effective mitigation of FO
224 membrane fouling. Variations of the normalized water flux for different fouling conditions were
225 consistent with the DGT adsorption efficiency (see for Fig. 3 (b)): indeed, there was no Ca^{2+}
226 adsorption for the single organic fouling while the DGT adsorption efficiency was ranged from 32.6%
227 to 62.8% for the enhanced organic fouling with different concentrations of Ca^{2+}. These results
228 implied that the DGT could effectively adsorb Ca^{2+} from the alginate bound foulants. As a result,
229 organic fouling of the FO membrane could be alleviated via the extraction of Ca^{2+} from the fouling
230 layer.

231 Fig. 3

232 Although the DGT could adsorb the Ca^{2+} from the fouling layer of the FO membrane, the
233 adsorption amount and efficiency were significantly influenced by adding concentration of Ca^{2+}.
234 DGT adsorption amount of Ca^{2+} correspondingly increased with the feed Ca^{2+} concentration (Fig.
235 3 (b)), which was driven by more Ca^{2+} binding with the alginate at a higher addition of Ca^{2+}.
236 However, the adsorption efficiency was enhanced from 1 to 15 mM Ca^{2+}, and started to decrease
237 when Ca^{2+} concentration reached 35 mM. Given that the DGT was constrained by adsorption
238 capacity, the decrease of adsorption efficiency at Ca^{2+} concentration of 35 mM could be attributed
239 to the saturation of DGT adsorption (0.59 ± 0.01 mg). Indeed, it was interesting that the DGT
240 adsorption efficiency was not correlated with the increase of the normalized water flux after the
241 DGT adsorption (Fig. 3 (a)), suggesting that the different structure and composition of the fouling
242 layer on the FO membrane surface at different fouling conditions might strongly affect the

mitigation of membrane fouling by the DGT adsorption. Thus, it is very necessary to further investigate the changes in structure and composition of the fouling layer before and after the DGT adsorption.

3.3 DGT adsorption altered fouling layer structure and improved cleaning efficiency

In order to evaluate the structure of fouling layer before and after DGT adsorption, the morphology, element composition and structure of fouled and DGT adsorbed FO membranes were analyzed by SEM, EDX and CLSM, respectively. The SEM images of the fouled FO membranes before and after the DGT adsorption are shown in Fig. 4. Compared with the SEM image of the virgin FO membrane (Fig. S3), a fouling layer was formed on the FO membrane surface when only sodium alginate was used. However, except for the fouling layer, some macromolecular biopolymers were appeared on the FO membrane surface in all scenarios with Ca^{2+} addition into the feed. More importantly, more macromolecular biopolymers deposited on the membrane surface with the increase of Ca^{2+} concentration. This result further demonstrated that Ca^{2+} enhanced the organic fouling and induced a severer FO membrane fouling. Noting that the high density "egg-box-shaped" gel networks were observed on the FO membrane surface when Ca^{2+} concentration increased to 35 mM. Correlation of foulant deposition amount on the FO membrane surface and the Ca^{2+} concentration observed from SEM images were consistent with the variations of the flux decline (Fig. 2). After the DGT adsorption, except for the single organic fouling induced by the sodium alginate (Fig. 4 (Aa) and Fig. 4 (Ba)), the deposition of alginate fouling layer on the FO membrane surface minimized regardless of the Ca^{2+} concentration, indicating the effective adsorption of Ca^{2+} from the fouling layer of the FO membrane by the DGT technology.

Fig. 4

From the EDX analyses, various elements including C, O, Na, S, Cl and Ca could be detected on the fouled FO membranes (Fig. S4 and Table S1). It was notable that the relative weight percentage of Ca on the fouled FO membranes correspondingly increased with the increase of the adding Ca^{2+} concentration, further indicating the occurrence of more severe "egg-box-shaped" gel networks on the FO membrane surfaces. After the DGT adsorptions, the relative weight percentage of Ca significantly reduced (Fig. S5 and Table S2). This result strongly proved the effective adsorption of Ca^{2+} from the fouling layer of the FO membrane by the DGT technology.

For further understanding the impacts of the DGT adsorption on the fouling structure of the FO membrane, the fouled FO membranes before and after the DGT adsorption were analyzed by the CLSM observations. From Fig. S6, all the fouled FO membrane surfaces were covered by polysaccharides, and these formed fouling layers were thick. The deposited polysaccharides slightly decreased for the fouling by both sodium alginate and Ca^{2+} after the DGT adsorption (Fig. S6 and Table 1). In addition, the porosity of the fouling layers induced by both the sodium alginate and Ca^{2+} significantly increased after the DGT adsorption (see for Table1). It has been demonstrated that the porosity significantly affects membrane fouling, i.e., less porosity results in a severe membrane fouling (Wu et al., 2009; Wang et al., 2018b). Thus, the mitigation of the fouling owing to both the alginate and Ca^{2+} by the DGT technology was mainly attributed to the fact that the structure of the fouling layer became more porous after the extraction of the organic-bound Ca^{2+}.

In order to further investigate whether DGT adsorption could enhance the physical cleaning, the fouled and DGT adsorbed FO membranes at the FS condition of sodium alginate and 35 mM Ca^{2+} were backwashed according to previous literature (Mi and Elimelech, 2010; Motsa et al., 2017). There was no significant variation of the normalized water flux for the fouled FO membrane after

287 the backwashing; by contrast, it significantly increased from 0.41 to 0.53 for the DGT adsorbed FO
288 membrane after backwashing (Fig. 5). It suggested that the DGT adsorption could enhance the
289 physical cleaning of the fouled FO membranes. Such evidence strongly suggested that the DGT
290 adsorption not only mitigated the FO membrane fouling but also enhanced the membrane cleaning
291 via changing the structure of the fouling layer.

292 Fig. 5

293 *3.4 Implications*

294 We demonstrated that the DGT technology can effectively alleviate organic fouling of FO
295 membranes via directly adsorbing Ca^{2+} from the fouling layer. The mechanisms on the *in situ*
296 mitigating FO membrane fouling are conceptualized in Fig. 6. With regard to a thick fouling layer
297 with alginate-Ca^{2+} gel networks, the Chelex resin in the DGT device can directly remove the
298 alginate-bound Ca^{2+} via the chelation of the Chelex functional groups. Due to the extraction of the
299 alginate-bound Ca^{2+} from the organic fouling layer, the structure of the fouling layer became more
300 porous and looser, which mitigated the FO membrane fouling and further enhanced the cleaning
301 efficiency. Moreover, the DGT devise can be reused for adsorbing Ca^{2+} after the resin layer was
302 regenerated by HNO_3 based on the results that the reused DGT device had a similar Ca^{2+} adsorption
303 amount compared with the new one. The success in alleviating organic fouling of the FO membrane
304 demonstrated the feasibility of fouling control strategy via directly extracting Ca^{2+} from the fouling
305 layer. Extracting the calcium from fouling layer played a critical role in altering membrane fouling
306 layer structure, which shed light on novel fouling control and management. However, applying such
307 DGT-based technique in controlling real FO membrane fouling still has limitations. On one hand,
308 the real FO fouling is composed of many other constituents such as precipitates, microorganisms,

and humic substances, which might disrupt the extraction of Ca^{2+} from the fouling layer. On the other hand, although the DGT technology was suitable for the flat-sheet FO membrane module applied in this study, it is difficult to directly apply in the spiral-wound or other tightly-packed membrane configurations. Thus, further studies should be focused on evaluating the DGT technology in real fouling scenarios where the co-existence of sparingly soluble inorganic minerals and organic foulants leads to a more complicated membrane fouling, and emphasized on developing other chelating agent or resin to replace with the DGT technology for in situ adsorbing calcium from the fouling layer in order to adapt to different foulants composition and membrane configurations.

Fig. 6

4. Conclusions

This study proposes a novel approach to mitigating the FO membrane fouling via the DGT for *in situ* removing Ca^{2+} binding with organic foulants. With regard to a thick fouling layer with alginate-Ca^{2+} gel networks, the Chelex resin in the DGT equipment can directly remove the organic-bound Ca^{2+} via the chelation. Owing to the extraction of the organic-bound Ca^{2+} from the membrane surface, the structure of the fouling layer became more porous and looser. The changes in the fouling structure alleviated the FO membrane fouling and further enhanced the cleaning effect. The success in mitigating the FO membrane fouling induced by the sodium alginate and Ca^{2+} demonstrated the feasibility of fouling controlling strategy via directly extracting Ca^{2+} from the fouling layer.

Acknowledgements

This work was supported by the National Natural Science Foundation of China [grant number 51578265]; the Six Major Talent Peaks of Jiangsu Province [grant number 2018-JNHB-014]; the Major Science and Technology Innovation Projects of Shandong Province [grant number

2018CXGC1006]; the Fundamental Research Funds for the Central Universities [grant number JUSRP 51728A]; and Jiangsu Cooperative Innovation Center of Technology and Material of Water Treatment.

Appendix A. Supplementary information

Detailed information on additional tables and figures can be found in the Supporting Information.

References

Arkhangelsky, E., Wicaksana, F., Tang, C.Y., Al-Rabiah, A.A., 2012. Combined organic-inorganic fouling of forward osmosis hollow fiber membranes. Water Res. 46 (19), 6329-6338.

Boo, C., Lee, S., Elimelech, M., Meng, Z.Y., Hong, S., 2012. Colloidal fouling in forward osmosis: Role of reverse salt diffusion. J. Membr. Sci. 390-391, 277-284.

Charfi, A., Jang, H., Kim, J., 2017. Membrane fouling by sodium alginate in high salinity conditions to simulate biofouling during seawater desalination. Bioresour. Technol. 240, 106-114.

Davison, W., Zhang, H., 2012. Progress in understanding the use of diffusive gradients in thin films (DGT) - back to basics. Environ. Chem. 9 (1), 1-13.

Degryse, F., Smolders, E., Zhang, H., Davison, W., 2009. Predicting availability of mineral elements to plants with the DGT technique: a review of experimental data and interpretation by modelling. Environ. Chem. 6 (3), 198-218.

Gu, Y.S., Wang, Y.N., Wei, J., Tang, C.Y., 2013. Organic fouling of thin-film composite polyamide and cellulose triacetate forward osmosis membranes by oppositely charged macromolecules. Water Res. 47, 1687-1874.

Guan, D.X., Williams, P.N., Luo, J., Zheng, J.L., Xu, H.C., Cai, C., Ma, L.N.Q., 2015. Novel

precipitated zirconia-based DGT technique for high-resolution imaging of oxyanions in waters and sediments. Environ. Sci. Technol. 49 (6), 3653-3661.

Kwan, S.E., Bar-Zeev, E., Elimelech, M., 2015. Biofouling in forward osmosis and reverse osmosis: Measurements and mechanisms. J. Membr. Sci. 493, 703-708.

Li, Q.L., Elimelech, M., 2006. Synergistic effects in combined fouling of a loose nanofiltration membrane by colloidal materials and natural organic matter. J. Membr. Sci. 278 (1), 72-82.

Liu, Y.L., Mi, B.X., 2012. Combined fouling of forward osmosis membranes: Synergistic foulant interaction and direct observation of fouling layer formation. J. Membr. Sci. 407-408, 136-144.

Luo, W.H., Phan, H.V., Xie, M., Hai, F.I., Price, W.E., Elimelech, M., Nghiem, L.D., 2017. Osmotic versus conventional membrane bioreactors integrated with reverse osmosis for water reuse: Biological stability, membrane fouling, and contaminant removal. Water Res. 109, 122-134.

Lutchmiah, K., Verliefde, A.R.D., Roest, K., Rietveld, L.C, Cornelissen, E.R., 2014. Forward osmosis for application in wastewater treatment: A review. Water Res. 58, 179-197.

Mi, B.X., Elimelech, M., 2008. Chemical and physical aspects of organic fouling of forward osmosis membranes. J. Membr. Sci. 320, 292-302.

Mi, B.X., Elimelech, M., 2010. Organic fouling of forward osmosis membranes: Fouling reversibility and cleaning without chemical reagents. J. Membr. Sci. 348 (1), 337-345.

McGinnis, R.L., Elimelech, M., 2007. Energy requirements of ammonia-carbon dioxide forward osmosis desalination. Desalination 207 (1), 370-382.

McGovern, R.K., Lienhard, J.H., 2014. On the potential of forward osmosis to energetically outperform reverse osmosis desalination. J. Membr. Sci. 469, 245-250.

Montero, N., Belzunce-Segarra, M.J., Gonzalez, J.L., Larreta, J., Franco, J., 2012. Evaluation of

375 diffusive gradients in thin-films (DGTs) as a monitoring tool for the assessment of the chemical
376 status of transitional waters within the Water Framework Directive. Mar. Pollut. Bull. 64 (1),
377 31-39.
378 Motsa, M.M., Mamba, B.B., Verliefde, A.R.D., 2015. Combined colloidal and organic fouling of
379 FO membranes: The influence of foulant-foulant interactions and ionic strength. J. Membr. Sci.
380 493, 539-548.
381 Motsa, M.M., Mamba, B.B., Thwala, J.M., Verliefde, A.R.D., 2017. Osmotic backwash of fouled
382 FO membranes: Cleaning mechanisms and membrane surface properties after cleaning.
383 Desalination 402, 62-71.
384 Mueller, L.N., de Brouwer, J.F.C., Almeida, J.S., Stal, L.J., Xavier, J.B., 2006. Analysis of a marine
385 phototrophic biofilm by confocal laser scanning microscopy using the new image
386 quantification software PHLIP. BMC Ecol. 6, 1-15.
387 Pendashteh, A.R., Fakhru'l-Razi, A., Madaeni, S.S., Abdullah, L.C., Abidin, Z.Z., Biak, D.R.A.,
388 2011. Membrane foulants characterization in a membrane bioreactor (MBR) treating
389 hypersaline oily wastewater. Chem. Eng. J. 168 (1), 140-150.
390 Perez, A.L., Anderson, K.A., 2009. DGT estimates cadmium accumulation in wheat and potato from
391 phosphate fertilizer applications. Sci. Total. Environ. 407 (18), 5096-5103.
392 Schintu, M., Marras, B., Durante, L., Meloni, P., Contu, A., 2010. Macroalgae and DGT as
393 indicators of available trace metals in marine coastal waters near a lead-zinc smelter. Environ.
394 Monit. Assess. 167 (1), 653-661.
395 Shaffer, D.L., Werber, J.R., Jaramillo, H., Lin, S.H, Elimelech, M., 2015. Forward osmosis: Where
396 are we now? Desalination 356, 271-284.

She, Q.H., Wang, R., Fane, A.G., Tang, C.Y., 2016. Membrane fouling in osmotically driven membrane processes: A review. J. Membr. Sci. 499, 201-233.

Sherwood, J.E., Barnett, D., Barnett, N.W., Dover, K., Howitt, J., Ii, H., Kew, P., Mondon, J., 2009. Deployment of DGT units in marine waters to assess the environmental risk from a deep sea tailings outfall. Anal. Chim. Acta. 652 (1-2), 215-223.

Siddiqui, F.A., She, Q.H., Fane, A.G., Field, R.W., 2018. Exploring the differences between forward osmosis and reverse osmosis fouling. J. Membr. Sci. 565, 241-253.

Sobeck, D.C., Higgins, M.J., 2002. Examination of three theories for mechanisms of cation-induced bioflocculation. Water Res. 36, 527-538.

Sun, Y., Tian, J.Y., Zhao, Z.W., Shi, W.X., Liu, D.M., Cui, F.Y., 2016. Membrane fouling of forward osmosis (FO) membrane for municipal wastewater treatment: A comparison between direct FO and OMBR. Water Res. 104, 330-339.

Tow, E.W., Lienhard, J.H., 2016. Quantifying osmotic membrane fouling to enable comparisons across diverse processes. J. Membr. Sci. 511, 92-107.

Town, R.M., Chakraborty, P., Van Leeuwen, H.P., 2009. Dynamic DGT speciation analysis and applicability to natural heterogeneous complexes. Environ. Chem. 6 (2), 170-177.

Van den Brink, P., Zwijnenburg, A., Smith, G., Temmink, H., Van Loosdrecht, M., 2009. Effect of free calcium concentration and ionic strength on alginate fouling in cross-flow membrane filtration. J. Membr. Sci. 345 (1), 207-216.

Wang, X.M., Waite, T.D., 2009. Role of Gelling Soluble and Colloidal Microbial Products in Membrane Fouling. Environ. Sci. Technol. 43 (24), 9341-9347.

Wang, Z.W., Ma, J.X., Tang, C.Y., Kimura, K., Wang, Q.Y., Han, X.M., 2014. Membrane cleaning

in membrane bioreactors: A review. J. Membr. Sci. 468, 276-307.

Wang, X.H., Chang, V.W.C., Tang, C.Y., 2016a. Osmotic membrane bioreactor (OMBR) technology for wastewater treatment and reclamation: Advances, challenges, and prospects for the future. J. Membr. Sci. 504, 113-132.

Wang, X.H., Zhao, Y.X., Yuan, B., Wang, Z.W., Li, X.F., Ren, Y.P., 2016b. Comparison of biofouling mechanisms between cellulose triacetate (CTA) and thin-film composite (TFC) polyamide forward osmosis membranes in osmotic membrane bioreactors. Bioresour. Technol. 202, 50-58.

Wang, X.H., Hu, T.Z., Wang, Z.W., Li, X.F., Ren, Y.P., 2017. Permeability recovery of fouled forward osmosis membranes by chemical cleaning during a long-term operation of anaerobic osmotic membrane bioreactors treating low-strength wastewater. Water Res. 123, 505-512.

Wang, X.H., Zhang, J.F., Chang, V.W.C., She Q.H., Tang C.Y., 2018a. Removal of cytostatic drugs from wastewater by an anaerobic osmotic membrane bioreactor. Chem. Eng. J. 339, 153-161.

Wang, W.Y., Yue, Q.Y., Li, R.H., Bu, F., Shen, X., Gao, B.Y., 2018b. Optimization of coagulation pre-treatment for alleviating ultrafiltration membrane fouling: The role of floc properties on Al species. Chemosphere 200, 86-92.

Wang, H.L., Wang, X.H., Meng, F.G., Li, X.F., Ren, Y.P., She, Q.H., 2019. Effect of driving force on the performance of anaerobic osmotic membrane bioreactors: New insight into enhancing water flux of FO membrane via controlling driving force in a two-stage pattern. J. Membr. Sci. 569, 41-47.

Warnken, K.W., Zhang, H., Davison, W., 2006. Accuracy of the Diffusive Gradients in Thin-Films Technique: Diffusive boundary layer and effective sampling area considerations. Anal. Chem.

78 (11), 3780-3787.

Wu, B., An, Y.Y., Li, Y.Z., Wong, F.S., 2009. Effect of adsorption/coagulation on membrane fouling in microfiltration process post-treating anaerobic digestion effluent. Desalination 242 (1), 183-192.

Xie, M., Nghiem, L.D., Price, W.E., Elimelech, M., 2013. Impact of humic acid fouling on membrane performance and transport of pharmaceutically active compounds in forward osmosis. Water Res. 47 (13), 4567-4575.

Yoon, H., Baek, Y., Yu, J., Yoon, J., 2013. Biofouling occurrence process and its control in the forward osmosis. Desalination 325, 30-36.

Yu, G.H., Tang, Z., Xu, Y.C., Shen, Q.R., 2011. Multiple fluorescence labeling and two dimensional FTIR-13C NMR heterospectral correlation spectroscopy to characterize extracellular polymeric substances in biofilms produced during composting. Environ. Sci. Technol. 45 (21), 9224-9231.

Yuan, B., Wang, X.H., Tang, C.Y., Li, X.F., Yu, G.H., 2015. In situ observation of the growth of biofouling layer in osmotic membrane bioreactors by multiple fluorescence labeling and confocal laser scanning microscopy. Water Res. 75, 188-200.

Zhang, H., Davison, W., 1995. Performance Characteristics of Diffusion Gradients in Thin Films for the in Situ Measurement of Trace Metals in Aqueous Solution. Anal. Chem. 67 (19), 3391-3400.

Zhang, H., Davison, W., Knight, B., McGrath, S., 1998. In Situ Measurements of Solution Concentrations and Fluxes of Trace Metals in Soils Using DGT. Environ. Sci. Technol. 32 (5), 704-710.

463 Zhang, H., Davison, W., 2015. Use of diffusive gradients in thin-films for studies of chemical
464 speciation and bioavailability. Environ. Chem. 12 (2), 85-101.
465 Zhao, S.F., Zou, L., Tang, C.Y., Mulcahy, D., 2012. Recent developments in forward osmosis:
466 Opportunities and challenges. J. Membr. Sci. 396, 1-21.
467 Zheng, L., Price, W.E., Nghiem, L.D., 2018. Effects of fouling on separation performance by
468 forward osmosis: the role of specific organic foulants. Environ. Sci. Pollut. R. 1-12.
469

Table Captions

Table 1 Structural parameters of fouling layer before and after DGT adsorption obtained from CLSM images via PHLIP[a].

Figure Captions

Fig. 1. Schematic view of the DGT adsorption device for the fouled FO membranes.

Fig. 2. Water flux profile of FO membranes during fouling filtration. FO fouling filtration was conducted with feed solution containing 200 mg/L sodium alginate, 20 mM NaCl, 20 mM Na_2SO_4 and 1 mM $NaHCO_3$, with varying calcium concentration from 1 to 35 mM. Draw solution was 4 M NaCl. The filtration was operated for 24 hours.

Fig. 3. DGT performance in fouling mitigation: (A) Normalized water flux and (B) DGT adsorption amount and efficiency at different fouling conditions. The FO fouling filtration conditions were described in Figure 2. DGT adsorption was performed using a DGT device with Chelex-100 strip, 1 M HNO_3 as the eluent. The error bar represents the standard deviation from three repeated experiments.

Fig. 4. SEM images of the fouled (A) and DGT adsorbed (B) FO membranes: (a) single organic fouling; (b) organic fouling + 1 mM Ca^{2+}; (c) organic fouling + 15 mM Ca^{2+}; (d) organic fouling + 35 mM Ca^{2+}.

Fig. 5. CLSM images of the fouled (A) and DGT adsorbed (B) FO membranes with alginate and 35 mM Ca^{2+} and normalized water flux before and after backwashing (C). Experimental condition for FO filtration was described in Figure 2, and DGT adsorption protocol was described in Figure 3.

Fig. 6. Mechanisms of Ca^{2+} adsorption from the fouling layer by the DGT technology.

492 Table 1 Structural parameters of fouling layer before and after DGT adsorption obtained

493 from CLSM images via PHLIP[a].

	Fouling layer	Average amount of polysaccharide ($\mu m^3\ \mu m^{-2}$)	Porosity (%)	Mean thickness (μm)
Before DGT adsorption	single organic fouling	12.25 ± 0.41	32.10 ± 4.70	24.85 ± 1.32
	organic fouling + 1 mM Ca^{2+}	13.00 ± 1.08	22.78 ± 7.54	24.81 ± 3.69
	organic fouling + 15 mM Ca^{2+}	14.06 ± 0.93	18.26 ± 9.46	26.26 ± 1.44
	organic fouling + 35 mM Ca^{2+}	14.13 ± 0.87	16.27 ± 0.80	25.56 ± 3.38
After DGT adsorption	single organic fouling	12.45 ± 0.05	35.06 ± 2.51	24.68 ± 3.26
	organic fouling + 1 mM Ca^{2+}	12.40 ± 0.09	33.49 ± 2.90	22.31 ± 0.95
	organic fouling + 15 mM Ca^{2+}	13.00 ± 0.19	28.14 ± 8.81	23.46 ± 0.29
	organic fouling + 35 mM Ca^{2+}	13.14 ± 0.26	20.86 ± 3.62	24.78 ± 0.49

494 [a] Values are given as mean values ± standard deviation (number of measurements: n=3). The

495 scanning area was 850 × 850 μm^2 in size.

496

497

498

499

500

501

502

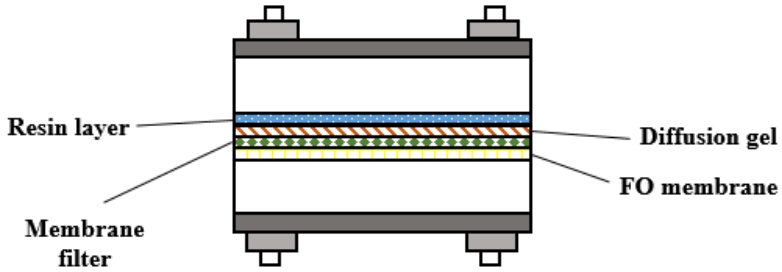

503

504 Fig. 1. Schematic view of the DGT adsorption device for the fouled FO membranes.

505

506

507

508

509

510

511

512

513

514

515

516

517

518

519

520

521

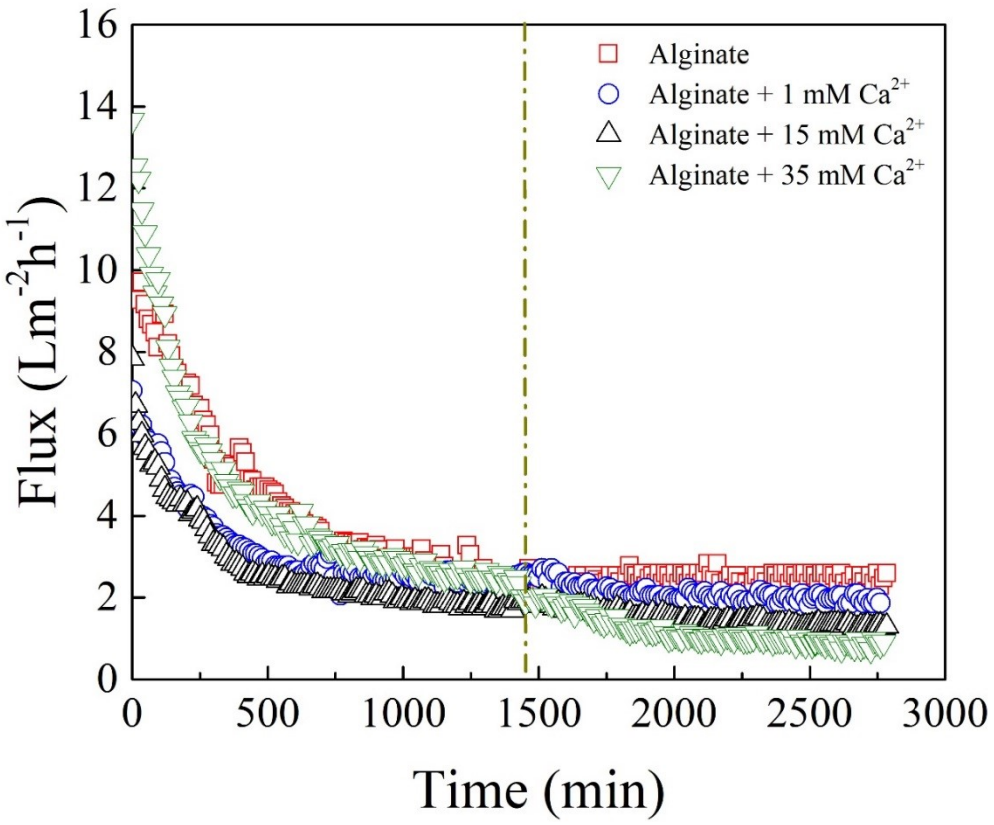

Fig. 2. Water flux profile of FO membranes during fouling filtration. FO fouling filtration was conducted with feed solution containing 200 mg/L sodium alginate, 20 mM NaCl, 20 mM Na_2SO_4 and 1 mM $NaHCO_3$, with varying calcium concentration from 1 to 35 mM. Draw solution was 4 M NaCl. The filtration was operated for 24 hours.

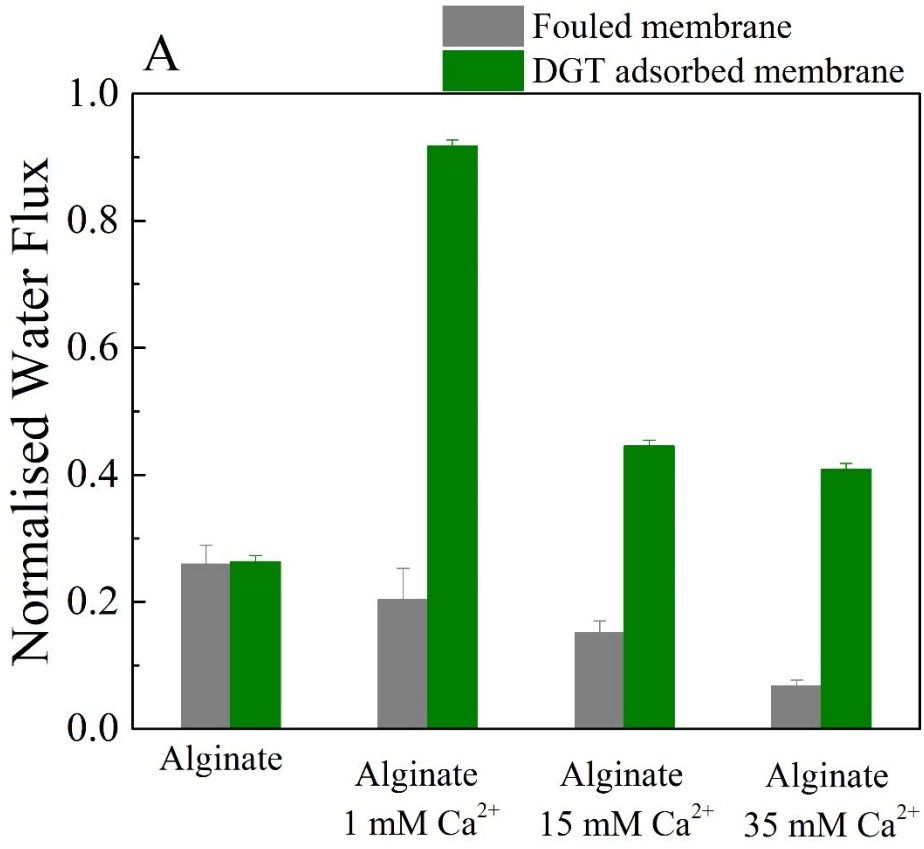

535

536

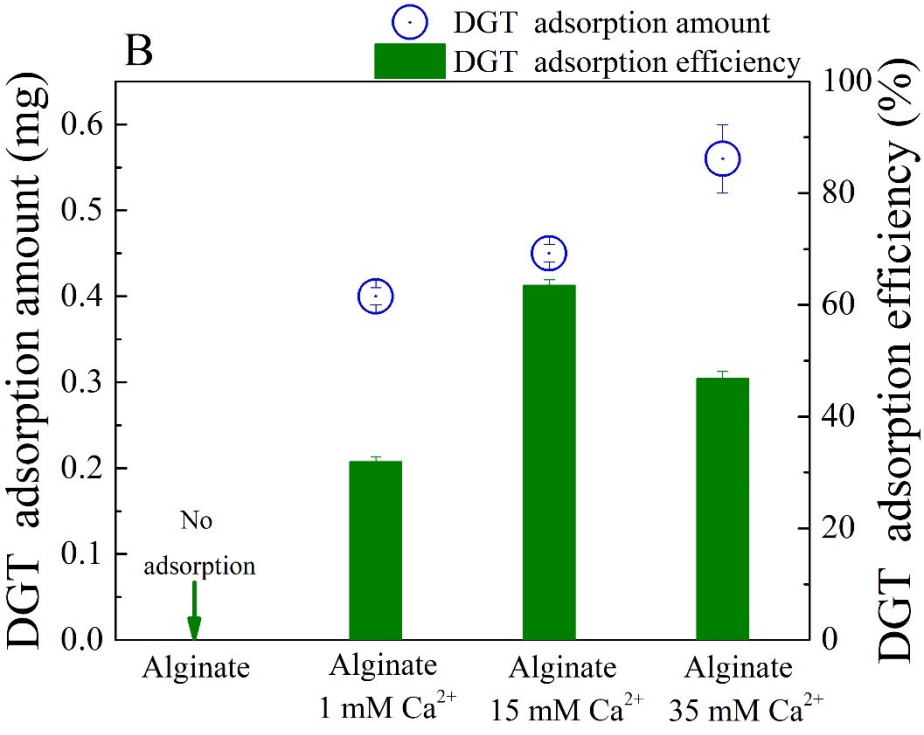

537

538 Fig. 3. DGT performance in fouling mitigation: (A) Normalized water flux and (B) DGT

539 adsorption amount and efficiency at different fouling conditions. The FO fouling filtration

conditions were described in Figure 2. DGT adsorption was performed using a DGT device with Chelex-100 strip, 1 M HNO_3 as the eluent. The error bar represents the standard deviation from three repeated experiments.

562 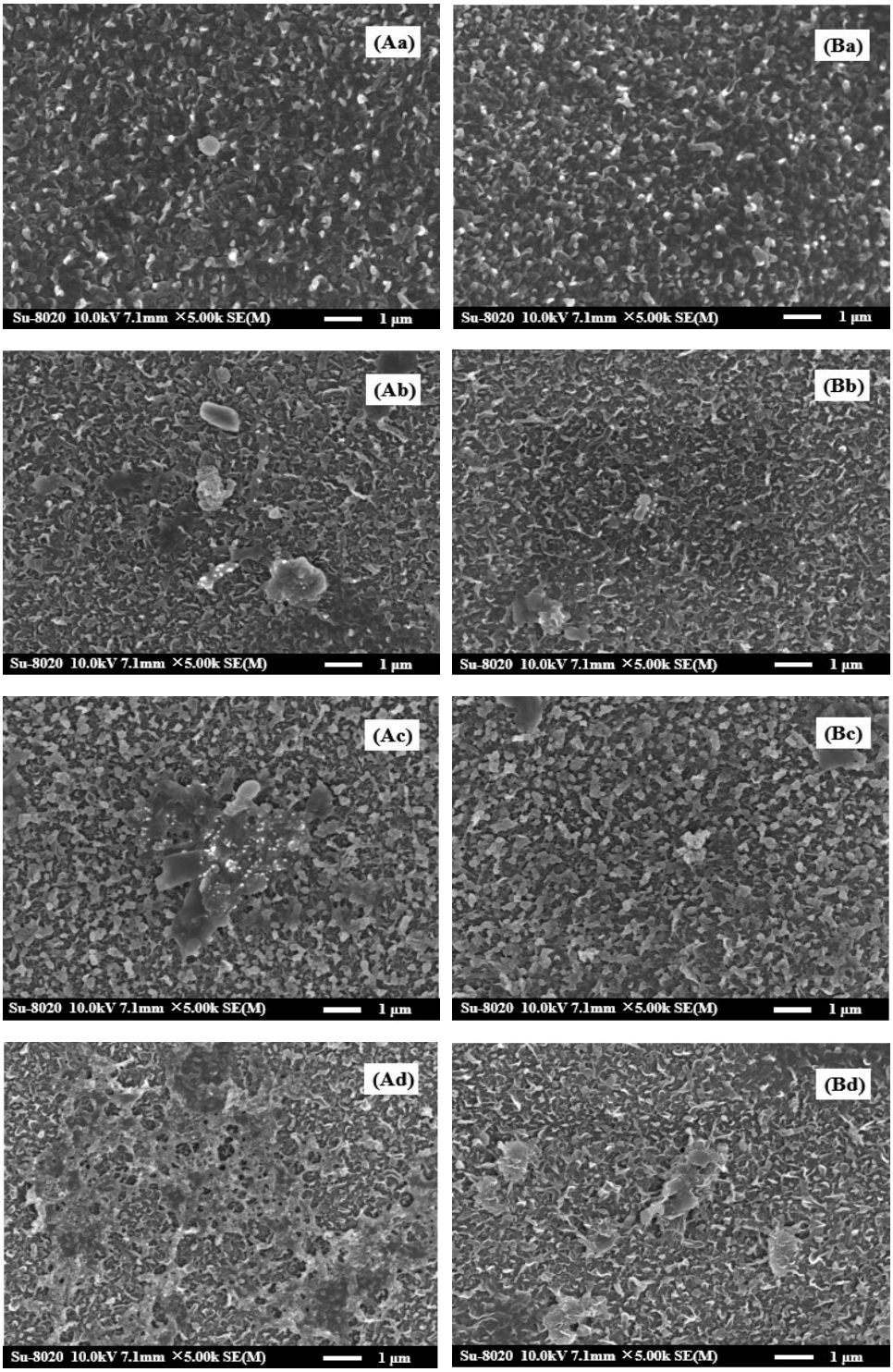

563
564
565

566 Fig. 4. SEM images of the fouled (A) and DGT adsorbed (B) FO membranes: (a) single organic

567 fouling; (b) organic fouling + 1 mM Ca^{2+}; (c) organic fouling + 15 mM Ca^{2+}; (d) organic fouling +

568 35 mM Ca^{2+}.

569

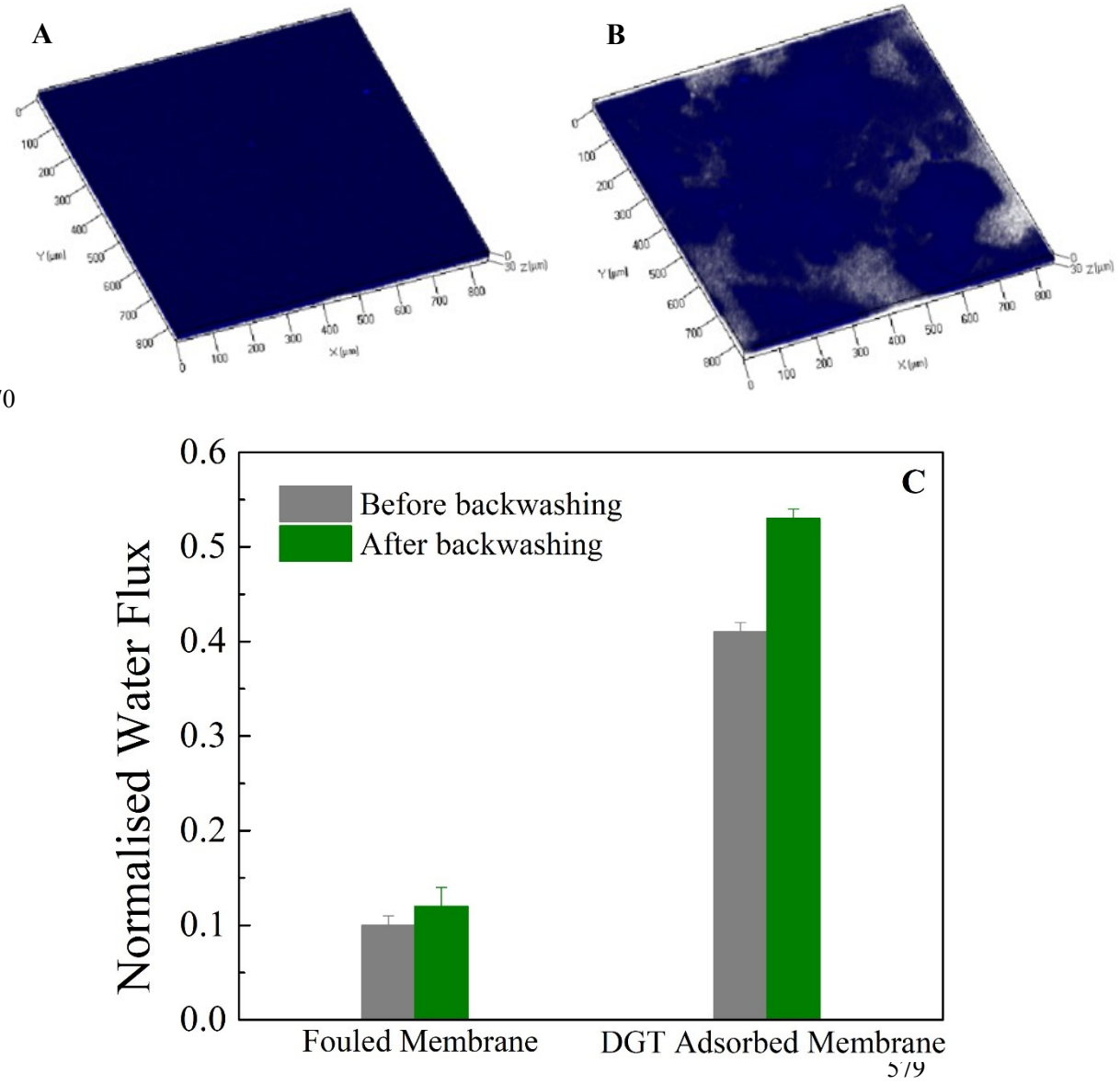

Fig. 5. CLSM images of the fouled (A) and DGT adsorbed (B) FO membranes with alginate and 35 mM Ca^{2+} and normalized water flux before and after backwashing (C). Experimental condition for FO filtration was described in Figure 2, and DGT adsorption protocol was described in Figure 3.

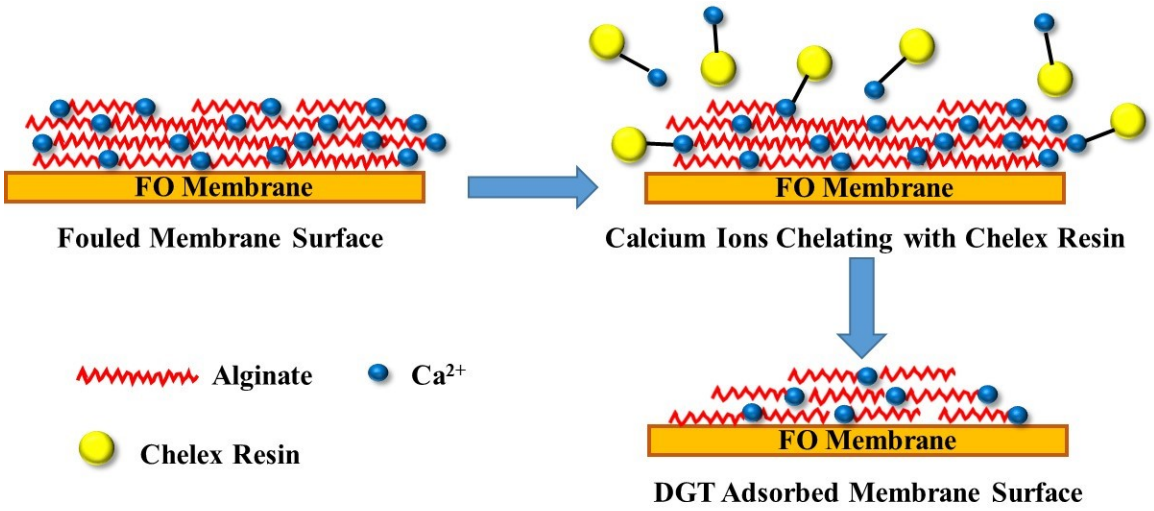

587

588 Fig. 6. Mechanisms of Ca^{2+} adsorption from the fouling layer by the DGT technology.